Journal of Composite Materials
http://jcm.sagepub.com

Optimisation of 3-D Lattice Cores in Composite Sandwich Structures

John T. Hwang *
Department of Aerospace Engineering, University of Michigan, USA

Craig A. Steeves
Institute for Aerospace Studies, University of Toronto, Canada

Abstract
Hybrid lattice cores for sandwich structures, containing both solid struts and polymer foam, are a recent option available to designers. These cores benefit from a synergistic effect in which the foam supports the slender struts against buckling in addition to carrying a portion of the applied loads directly. This work will optimise these hybrid cores to minimize unit cell density given compressive and shear strength constraints for a variety of unit cell configurations. An analytical model is developed for prediction of failure using the assumption that the foam is an elastic foundation that supports the struts; however, the unit cells are found to be optimal when no polymer foam is used. With the problem thereby simplified, analytical optimisation solutions are derived and studied extensively, revealing qualitative insights about efficient lattice core designs. Optimal strut inclination angle, failure mode, and configuration are plotted against loading, which reveal that, for the large majority of strength constraints, the lowest unit cell density is achieved with tetrahedral cores whose struts fail in compressive yielding.

Keywords
optimisation; sandwich structures; analytical modeling; buckling; composite materials

* Corresponding author: hwangjt@umich.edu

1. Introduction

Sandwich structures have been used for nearly two centuries for applications requiring high bending stiffness [1, 2, 3]. Traditionally, balsa, foam, or honeycomb cores are surrounded by stiff face sheets, yielding a lightweight plate or beam that is efficient in bending. Though this design can have high specific strength, there are disadvantages to each of these material options: foam and balsa are stochastic materials and therefore relatively inefficient, while honeycomb adheres poorly to the face sheets because of the small bond area and has issues with water ingress.

Options for addressing these weaknesses include pin reinforcement [4] and lattice cores [5, 6]. Pin reinforcement involves inserting pins into foam in a regular geometric pattern, typically forming disjunct pyramids, and then adhering face sheets to the pin-reinforced foam [7]. Lattice cores use metallic periodic structures formed through perforation and bending [8]. The pore spaces can optionally be filled with foam after assembly of the sandwich [9] to form a foam-strut hybrid. The combination of polymer foam and reinforcing struts increases the compressive and shear strengths of the core material and has a symbiotic effect because the polymer foam reduces the propensity of the slender struts to buckle. The added complexity of both the pin-reinforced and lattice cores offers greater design freedom that can be used to tailor the cores for acoustic performance [10], impact resistance [11], active cooling [12], thermal insulation [13], or fatigue mitigation [14].

Before addressing issues of multifunctionality, a fundamental question is the optimal design for pin-reinforced or lattice cores which has the minimum mass for a required strength. There are many examples in the literature involving design optimisation of a sandwich plate or beam subject to failure constraints [15, 16, 17, 18, 19]. Sandwich beams in bending fail in one of four modes: face yield, face wrinkling, core shear, and indentation [5]. However, only the last two pertain to the core — indentation is due to locally large compressive stresses near the points of concentrated loading that are transmitted to the core, and core shear is direct shear failure of the core material.

The design problem can be simplified because core compressive and shear strength can be considered to be independent of the face sheets. Thus, a unit cell of the core can be optimised to provide a necessary combination of shear strength and compressive strength for a minimum density to withstand the local stresses. Since only the core is considered as opposed to the full sandwich structure, core thickness is removed from the problem by using only non-dimensional geometric design variables. Dragoni [20] used analytical methods to minimize the mass of tetrahedral-core sandwich panels subject to bending. Here, the local problem of optimization of a unit cell is considered, which will enable minimum mass graded truss-core sandwich structures.

Unlike previous work, the approach taken here is to parametrize the core as a foam-strut hybrid with foam density and lattice geometry as variables so that a pure foam core and a pure lattice core are captured within the design space. Furthermore, this study will address several unanswered questions including a quantitative comparison among lattice configurations and among foam, lattice, pin-reinforced, and hybrid cores, as well as a detailed examination of the impact of the loading on the optimal lattice geometry of the

Fig. 1. Unit cells of each configuration with the foam removed for clarity.

core and the failure mode of the struts. The design heuristics and quantitative results produced by such a study can be used in the design of a plate or a beam by choosing the optimal core configuration for each section of the sandwich structure based on the local compressive and shear stresses the core must carry.

This paper will derive the models needed to predict the shear and compressive strengths of hybrid unit cells as functions of the unit cell geometry and the material properties. The models will be used to find minimum mass designs with respect to the overall strut configuration (pyramidal, tetrahedral), the strut radius and inclination, and the density of the foam.

2. Unit Cell Configurations

2.1. Geometry

Three configurations of unit cells of struts immersed in polymer foam will be examined. These configurations, shown in Figure 1, will be referred to as: pinned, pyramidal and tetrahedral. The first is fabricated using a pinning process [4, 21] while the remaining two are manufactured by the forming process detailed in [8]. There are two relevant differences between the formed and pinned unit cells. First, for the formed configurations the unit cell width is fully determined by the strut angle and the unit cell height, while for the pinned geometries, because the pins need not meet at their ends the unit cell width is independent of the other parameters. Second, rotation at the strut ends is more constrained for the formed unit cells than the pinned unit cells which has implications for the analysis of strut buckling. For the pyramidal configuration, the struts are arranged such that they form the oblique sides of a square-based pyramid. The pinned configuration has a similar arrangement, but the in-plane spacing among struts is allowed to vary provided the square base and the symmetrical arrangement of the four struts are maintained. Similarly, for the tetrahedral configuration the struts form the oblique sides of a tetrahedron with an equilateral triangle as the base.

The relevant geometric variables are strut radius a, unit cell thickness c, and strut inclination angle ω. The strut inclination angle ω is defined with respect to the vertical axis of the unit cell, as shown in Figure 2. The unit cell width, d, is a fourth independent variable that applies only in the case of the pinned configuration since the spacing between each distinct set of pins can be set arbitrarily. The volume

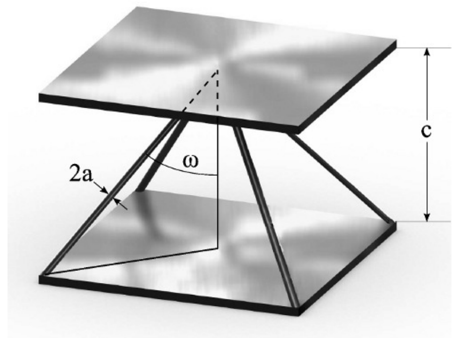

Fig. 2. The geometry of the solid constituents of the unit cell with the foam removed. The relevant variables are the strut radius a, the unit cell thickness c, and the angle of inclination of the struts ω, which are shown for a pyramidal unit cell.

fraction of the unit cell is defined as the ratio between the volume of the struts in a unit cell and the total volume of the unit cell. For the pyramidal and tetrahedral configurations, the expression for unit cell base area accounts for the strut radius at the joints, in addition to dependence upon the unit cell thickness c and the strut inclination ω, in order to avoid zero volumes and infinite volume fractions for unit cells with vertical pins (that is, $\omega = 0$).

2.2. Materials

The unit cells are composed of solid strut material with polymer foam in the interstices between the struts. For the results presented in this paper, the strut material is annealed titanium alloy Ti-6Al-4V (Grade 5), which has density 4430 kg/m^3, Young's modulus 114 GPa and yield strength 880 MPa (data source: www.matweb.com). Pultruded carbon fibre, aluminum alloy Al 7075-T6, 304 stainless steel, and Inconel 600 were also considered, but the qualitative conclusions were found to be unaffected by switching to these materials.

The void space between the struts is filled with polymer foam. The relevant material properties of the polymer foam are the Young's modulus E_f and the shear modulus G_f, which are both functions of the foam relative density $\bar{\rho} = \rho_f/\rho_p$, where ρ_f is the foam density and ρ_p is the density of the parent solid polymer. Following the approximations from [22], the polymer foam moduli are assumed to be quadratic in the foam relative density:

$$E_f = k_E \bar{\rho}^2 E_p \tag{1}$$

$$G_f = k_G \bar{\rho}^2 E_p, \tag{2}$$

where k_E and k_G are the coefficients of proportionality for Young's modulus and shear modulus, respectively, and E_p is the Young's modulus of the solid polymer of which the foam is composed. Two standard foams are Divinycell H-grade (parent material polyvinyl chloride of density 1390 kg/m^3 and Young's modulus 4 GPa) and Rohacell aircraft-grade (parent material polymethacrylimide of density 1200 kg/m^3 and Young's modulus 2.5 GPa [23]). The values of the coefficients, computed from data obtained from the manufacturers, are $k_E = 2.828$ and $k_G = 0.969$ for Divinycell and $k_E = 8.280$ and $k_G = 2.573$ for Rohacell. The results presented henceforth assume strictly Rohacell as the foam material as the stiffnesses and yield strengths of the two foams are within 30% of each other in the range of foam densities considered — between 0 kg/m^3 and 250 kg/m^3 — and do not affect the qualitative results of this paper.

3. Analysis

The following development of the unit cell strength model consists of two parts. First is the analysis of the unit cell, to determine the stresses induced in the struts by applied compression and shear. Because the yield strains of the foams are generally much larger than the yield strains of the strut materials, the peak load that the unit cell can carry is determined by failure of one or more struts. Strut failure is determined by tensile or compressive yielding, or by elastic buckling. Second is an explanation of the strut buckling model. The elastic buckling of a strut immersed in an elastic medium is of particular interest because the primary justification for inserting the foam is that it delays or suppresses strut buckling.

3.1. Elastic stress analysis of the unit cells

The compressive and shear stresses applied to the unit cell are carried by the struts and foam, both of which are linear elastic. The distribution of internal stresses is determined by requiring compatibility of displacements in the struts and foam; the degrees of freedom are the x and z displacements of the upper surface relative to the lower one. The surfaces are assumed to be infinitely rigid and thus the two displacements fully define the deflected state of the unit cell. Figure 3 illustrates the coordinate system, strut nomenclature, and applied loads for each configuration.

Application of combined compressive stress σ and shear stress τ to the unit cell induces the following internal stresses: foam compressive and shear stresses σ_f and τ_f, respectively, and axial stresses σ_1 and σ_2 in the struts. All normal stresses are defined positive in compression since tensile loading of the unit cell is not considered in this work. In terms of these quantities, volume fraction f, and strut inclination angle ω, equilibrium in the vertical and horizontal directions yields

$$\sigma = \frac{C_1}{n} f \cos^2 \omega \sigma_1 + \frac{C_2}{n} f \cos^2 \omega \sigma_2 + \sigma_f \tag{3}$$

$$\tau = \frac{C_3}{n} f \cos \omega \sin \omega \sigma_1 - \frac{C_3}{n} f \cos \omega \sin \omega \sigma_2 + \tau_f, \tag{4}$$

where n represents the number of struts in a unit cell of the given configuration, and C_1, C_2, and C_3 are other configuration-dependent constants that are presented in Table 1.

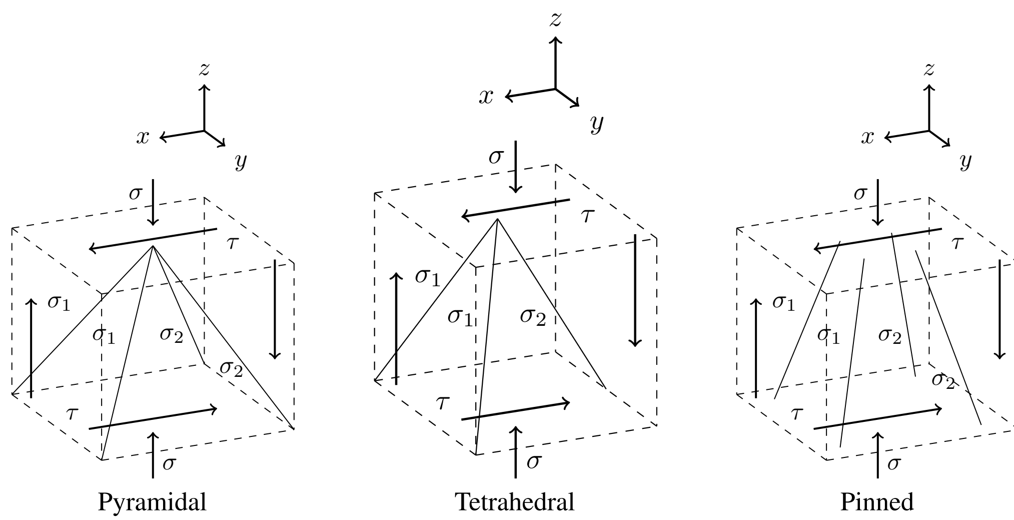

Fig. 3. Coordinate system and nomenclature for each unit cell configuration.

The relevant elastic constants are the Young's modulus of the strut E_s, the Young's modulus of the foam E_f, and the shear modulus of the foam G_f. Using these constants and linearized strain-displacement relations, σ and τ can be expressed in terms of the x and z displacements, δ_x and δ_z. Inverting this 2×2 system gives δ_x and δ_z explicitly in terms of the applied stresses σ and τ. Finally, δ_x and δ_z can be inserted into the equations for σ_1 and σ_2 to arrive at expressions for the internal stresses in the struts in terms of the applied stresses:

$$\begin{aligned}\sigma_{1,2} = &\left(\frac{\cos^2\omega}{\frac{C_1+C_2}{n} f \cos^4\omega + \frac{E_f}{E_s}} \right)\sigma \pm \left(\frac{C_{4,5}\cos\omega\sin\omega}{\frac{C_3(C_4+C_5)}{n} f\cos^2\omega\sin^2\omega + \frac{G_f}{E_s}} \right)\tau \\ &- \left(\frac{\frac{C_1C_4-C_2C_5}{n} f\cos^5\omega\sin\omega}{\left[\frac{C_1+C_2}{n} f\cos^4\omega + \frac{E_f}{E_s}\right]\left[\frac{C_3(C_4+C_5)}{n} f\cos^2\omega\sin^2\omega + \frac{G_f}{E_s}\right]} \right)\tau, \end{aligned} \tag{5}$$

where C_4 and C_5 are constants introduced to simplify the expressions and are listed in Table 1. Note that the foam properties E_f and G_f are functions of the foam relative density $\bar{\rho}_f$ as indicated in Equations (1) and (2).

	n	C_1	C_2	C_3	C_4	C_5
Pyramidal	4	2	2	$\sqrt{2}$	$\frac{1}{\sqrt{2}}$	$\frac{1}{\sqrt{2}}$
Tetrahedral	3	2	1	1	$\frac{1}{2}$	1
Pinned	4	2	2	$\sqrt{2}$	$\frac{1}{\sqrt{2}}$	$\frac{1}{\sqrt{2}}$

Table 1: Values of the constants appearing in the unit cell analysis, listed for each configuration.

3.2. Strut Buckling

3.2.1. Foundation Modulus The total load necessary to cause the elastic buckling of a strut is increased when the transverse deformation of the strut is resisted. In the case of a strut-foam hybrid, resistance is provided by the polymer foam, which acts as an elastic foundation. To obtain a closed form analytical solution for the buckling load, the method of [24] is employed, assuming that the effective spring constant of the foam per unit length along the strut is constant. This constant is the foundation modulus, β, determined by the unit cell geometry and the material properties of the foam. The use of the foundation modulus is valid if the foam displays a linear elastic response to the deflected pin. Cartié and Fleck [4] examine the compressive stress response for a low density Rohacell foam, and show that the foam is linear only for very small strains ($< 2\%$) followed by a long yield plateau at constant stress. For unit cells with a large proportion of solid strut material (which will be the case for large strut radii or small inclination angles) the strains in the foam caused by the deflected pins can exceed this limit, at which point the use of an elastic foundation modulus overestimates the ability of the foam to delay strut buckling. This problem can be obviated by using a combined elastic-plastic model [25, for example], but at a large increase in complexity. The elastic foundation approximation obtains a closed form solution which is advantageous for use in optimisation.

The interaction of the strut and the foam can be approximated as an elastic beam upon a foundation comprised of adjacent elastic springs where the foundation modulus can be expressed as a function of the foam stiffness, with the length of the springs unknown:

$$\beta = \frac{k}{L} = \frac{E_f A}{sL} = \frac{2E_f aL}{sL} = \frac{2E_f a}{s}, \tag{6}$$

where L is the strut length, k is the spring constant, s is the spring length, and A is the area of the strut projected onto the plane normal to its transverse deflection. The foam supports the strut only from the side to which the strut is deflected as the struts are not bonded to the foam. Liu et al. [26] model the foundation as the superposition of vertical and horizontal springs; the unit cell height and width are used as the spring lengths in the vertical and horizontal directions respectively. However, the struts need not deflect parallel to the unit cell sides and hence the unit cell width is an underestimation of the average horizontal spring length, which makes this technique slightly unconservative. The horizontal distance to the unit cell boundary is a function of both vertical position along the strut and the direction of buckling. For an arbitrary location on a strut, the horizontal distances to the unit cell boundaries are, on average, half the unit cell width. The average horizontal spring length can be determined by calculating the average distance from the centroid to the boundary of the square or rectangle, when viewed from above. If $\sqrt{2}c\tan\omega$ is the side length of the square unit cell base, the average horizontal spring length for the pyramidal core is

$$s = \frac{4\sqrt{2}}{\pi}\ln(1+\sqrt{2})c\tan\omega \approx 1.1222\sqrt{2}c\tan\omega, \tag{7}$$

and for the tetrahedral unit cell the average horizontal spring length is

$$s = 2 \times 0.8845c \tan \omega \tag{8}$$

(The analytical expression is omitted for the sake of brevity). With the spring lengths known, the foundation modulus can be calculated as the net resultant from the horizontal and vertical springs. The expressions for the pinned, pyramidal, and tetrahedral configurations are, respectively:

$$\beta = \frac{2E_f a}{c} \sin \omega + \frac{2E_f a}{1.1222d} \cos \omega, \tag{9}$$

$$\beta = \frac{2E_f a}{c} \sin \omega + \frac{2E_f a}{1.1222\sqrt{2}c \tan \omega} \cos \omega, \tag{10}$$

and

$$\beta = \frac{2E_f a}{c} \sin \omega + \frac{2E_f a}{1.7690c \tan \omega} \cos \omega, \tag{11}$$

3.2.2. Strut Buckling Load The critical buckling load, P_{cr}, for a simply supported beam on an elastic foundation is derived by [24]:

$$P_{cr} = \frac{\beta L^2}{m^2 \pi^2} + \frac{m^2 \pi^2 EI}{L^2}, \tag{12}$$

where E is the Young's modulus of the beam material, I is the second moment of area of the beam, L is the length of the beam and m is the number of half sine waves over which the beam buckles.

According to [4], the struts in the hybrid behave with restraint intermediate between simply supported and rigidly connected. Here the critical buckling load is found for a beam with clamped ends using an approach similar to the one used by [24]. The transverse deflection, y, is a function of the position along the beam, x. For the simply supported beam the deflected shape is a Fourier sine series, but the built-in beam necessitates a cosine series form:

$$y = \sum_{m=1}^{\infty} a_m \left(1 - \cos \frac{m\pi x}{L}\right). \tag{13}$$

The external work done by the buckling load is equated to the total internal energy in the strut and foam resulting from the strain response that satisfies equilibrium:

$$U_{ext} = U_{int} = U_{strut} + U_{foam}. \tag{14}$$

Assuming small displacements, inserting expressions for each term in terms of the deflection curves yields

$$\frac{P_{cr}}{2} \int_0^L \left(\frac{\mathrm{d}y}{\mathrm{d}x}\right)^2 \mathrm{d}x = \frac{EI}{2} \int_0^L \left(\frac{\mathrm{d}^2 y}{\mathrm{d}x^2}\right)^2 \mathrm{d}x + \frac{\beta}{2} \int_0^L y^2 \, \mathrm{d}x, \tag{15}$$

and inserting the cosine series approximation for y yields

$$P_{cr} = \frac{\sum_{m=1}^{\infty}\left[\frac{16EIm^4\pi^4}{L^4}a_m^2 + 2\beta a_m\left(\sum_{n=1}^{\infty} a_n\right) + \beta a_m^2\right]}{\sum_{m=1}^{\infty} 4\frac{m^2\pi^2}{L^2}a_m^2}. \tag{16}$$

It is possible to show that if all the Fourier coefficients are constrained to be non-negative, P_{cr} is minimized by the choice that all coefficients except one are zero.

To prove this, take $a_i = 0, \forall i \neq m$, so $\mathbf{a} = (0, \cdots, a_m, \cdots, 0)$. Then,

$$P_{cr}|_{a_m} = \frac{\frac{16EIm^4\pi^4}{L^4}a_m^2 + 3\beta a_m^2}{4\frac{m^2\pi^2}{L^2}a_m^2}. \tag{17}$$

Here, m is chosen such that the above expression for P_{cr} is as small as possible. Now, take any other coefficient, a_n, and make it non-zero as well so that $\mathbf{a} = (0, \cdots, a_m, \cdots, a_n, \cdots, 0)$. Then,

$$P_{cr}|_{a_m,a_n} = \frac{\left(\frac{16EIm^4\pi^4}{L^4}a_m^2 + 3\beta a_m^2\right) + \left(\frac{16EIn^4\pi^4}{L^4}a_n^2 + 3\beta a_n^2\right) + 4\beta a_m a_n}{\left(4\frac{m^2\pi^2}{L^2}a_m^2\right) + \left(4\frac{n^2\pi^2}{L^2}a_n^2\right)}. \tag{18}$$

If the $4\beta a_m a_n$ term is ignored temporarily, the expression in Eq. (18) can be viewed as the numerator and denominator of $P_{cr}|_{a_n}$ added to the numerator and denominator, respectively, of $P_{cr}|_{a_m}$ (Eq. (17)). Adding the numerators and denominators of two fractions yields a quotient less than the larger of and greater than the smaller of the two original quotients, and $P_{cr}|_{a_m} < P_{cr}|_{a_n}$ by construction. Thus, $P_{cr}|_{a_m,a_n}$ without the $4\beta a_m a_n$ term is larger than $P_{cr}|_{a_m}$ and adding this additional positive term only increases the difference. It is easy to see that additional non-zero coefficients cannot decrease P_{cr} below $P_{cr}|_{a_m}$, so this proves that $\mathbf{a} = (0, \cdots, a_m, \cdots, 0)$ for the right choice of m minimizes P_{cr}.

Simplifying Eq. (17) yields the following expression for the critical buckling load with clamped supports which is similar in form to the simply supported buckling load, but is only an approximation in this case:

$$P_{cr} = \frac{3\beta L^2}{4m^2\pi^2} + \frac{4m^2\pi^2 EI}{L^2}. \tag{19}$$

The key steps in this derivation are the use of the cosine series basis, which only permits symmetric buckling modes, and the assumption that all coefficients must be positive. Both have the effect of artificially stiffening the beam, yielding an upper bound for the critical buckling load that becomes less accurate with increasing foundation modulus. However, Eq. (19) is very accurate for small foundation moduli, specifically while the first buckling mode is the active one, and it is a simple equation that is easily evaluated whereas the exact solution is an implicit equation [27]. Much of the hybrid core designs of interest lie in this region where the foam is compliant enough that the struts buckle in a single cosine wave-like manner. Furthermore, it is shown in the next section that optimal cores for the load cases considered do not have any foam even with the overprediction of the strut buckling load, so the error in this model does not adversely affect the final results of this paper.

For convenience, Equations (12) and (19) are unified to yield a single equation in terms of a parameter, e, which must be set to 1 for pin jointed and 4 for clamped end conditions. For formed configurations — pyramidal and tetrahedral — clamped end conditions are more appropriate because the struts are assembled with solid joints prior to the insertion of foam. In contrast, pins are more compliant in rotation at their ends. Thus, the optimisation results that follow use $e = 1$ for the pinned configuration and $e = 4$ for the remaining configurations.

3.3. Effect of transverse loading on the struts

The unit cell analysis presented in Sec. 3.1 proceeds under the assumption that the struts carry only axial loads. The justification for this assumption is the struts' low stiffness with respect to transverse deformation compared to the axial stiffness of the other struts. This assumption leads to the adoption of Euler buckling formulae (plus additional terms to model the foam), but the claim that this buckling model is valid in the presence of transverse loading merits further investigation.

For the purposes of this discussion, the foam is ignored both for convenience and because it is shown in Sec. 4.1 that optimal cores do not have any foam. For each strut in compression, the external loads acting on it are decomposed into an axial force and a shear load at one end with the other end clamped. The next step is to assume that there are many unit cells distributed across the sandwich beam in the direction of bending, so the relative rotation of the upper and lower face sheets can be assumed to be zero. This translates into fixed-rotation boundary conditions for the strut analysis. The stiffness of the other struts is captured using a linear spring that provides resistance to transverse deflection at the vertically free end of the strut. Thus, the strut is modeled as a beam with length L and bending stiffness EI that is clamped at one end and free to deflect but not rotate at the other end, with axial and transverse loads P and Q, respectively, and a vertical spring with stiffness k.

With no distributed loading, the governing equation for the beam is

$$\bar{w}'''' + \lambda^2 \bar{w}'' = 0 \tag{20}$$

where $\lambda^2 \equiv \frac{PL^2}{EI}$ and the bar signifies normalization, and the general solution is

$$\bar{w}(\bar{x}) = A_1 \cos \lambda \bar{x} + A_2 \sin \lambda \bar{x} + A_3 \bar{x} + A_4 \tag{21}$$

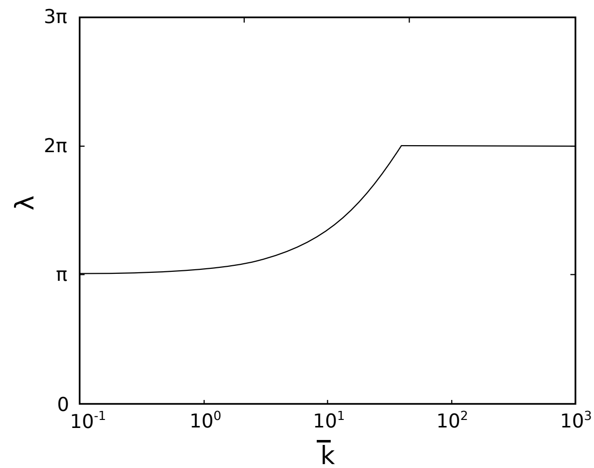

Fig. 4. Plot showing the dependence of the critical buckling load on the spring stiffness.

The kinematic boundary conditions are $\bar{w}(0) = 0$, $\bar{w}'(0) = 0$, and $\bar{w}'(1) = 0$, and there is a shear boundary condition at the tip given by

$$\bar{w}'''(1) - \bar{k}\bar{w}(1) = -\bar{Q} \tag{22}$$

with $\bar{k} \equiv \frac{kL^3}{EI}$ and $\bar{Q} \equiv \frac{QL^2}{EI}$.

Applying the boundary conditions yields the following linear system:

$$\begin{bmatrix} 1 & 0 & 0 & 1 \\ 0 & \lambda & 1 & 0 \\ -\lambda\sin\lambda & \lambda\cos\lambda & 1 & 0 \\ \lambda^3\sin\lambda - \bar{k}\cos\lambda & -\lambda^3\cos\lambda - \bar{k}\sin\lambda & -\bar{k} & -\bar{k} \end{bmatrix} \begin{bmatrix} A_1 \\ A_2 \\ A_3 \\ A_4 \end{bmatrix} = \begin{bmatrix} 0 \\ 0 \\ 0 \\ -\bar{Q} \end{bmatrix} \tag{23}$$

As λ approaches a value that makes the matrix singular, the solution to Eq. (23) grows without bound. The lowest of such values of λ corresponds to the critical buckling load, and it is dependent on the spring stiffness constant. As Figure 4 shows, the critical value of λ varies between π and 2π. When $\bar{k}$ is 0, λ is equal to π, so the buckling load is $\pi^2 EI/L^2$, as expected. As the spring constant increases, the critical λ also increases until $\bar{k} = 4\pi^2$ when λ is 2π, yielding a buckling load of $4\pi^2 EI/L^2$. Above $\bar{k} = 4\pi^2$, the spring is sufficiently stiff that it behaves like a clamped restraint, which is equivalent to the limiting case of an infinitely stiff spring.

The fact that this transition occurs at $\bar{k} = 4\pi^2$ can be explained by examining the determinant of the matrix in Eq. (23) and treating it as a function that implicitly determines λ:

$$\det[\cdot] = \lambda[2\bar{k}(\cos\lambda - 1) + \lambda\bar{k}\sin\lambda - \lambda^3\sin\lambda] \tag{24}$$

This equation always has the root of $\lambda = 2\pi$, but for $\bar{k} < 4\pi^2$, this equation has another non-trivial root that is strictly less than 2π. The latter root disappears and 2π becomes the smallest root when $\partial(\det[\cdot])/\partial\lambda = 0$ at $\lambda = 2\pi$; this condition is satisfied when $\bar{k} = 4\pi^2$.

The spring constant is assumed to be $k = \alpha E_s A/L$ where α is a scaling factor that takes into consideration the fact that the other struts in the unit cell are not perpendicular to the beam in the plane of the applied shear load. Since $\bar{k} = kL^3/E_s I$, inserting the above expression for k and simplifying yields

$$\bar{k} = \frac{4\alpha}{\bar{a}^2\cos^2\omega} \tag{25}$$

Since $\bar{a}$ is typically $O(\sim 10^{-2})$, $\bar{k}$ is well above $4\pi^2$. There is potential for α to be small when the struts are nearly vertical but this is only the case when the loading on the unit cell is predominantly compressive. Thus, for relevant unit cell geometries and load cases, the critical value of λ is 2π, so modeling the strut bucking load as $4\pi^2 EI/L^2$ is valid.

4. Optimisation

The geometric variables are non-dimensionalized with respect to core thickness c, stress variables and moduli are non-dimensionalized with respect to the strut axial modulus E_s, and densities are non-dimensionalized with respect to strut material density ρ_s. The resulting equations for the unit cell geometry and strut buckling analysis are shown in Table 2.

The optimisation problem is a nonlinear, constrained minimisation problem with non-dimensional unit cell density as the objective function. The design variables are the strut radius $\bar{a}$, foam density $\bar{\rho}_f$, and strut inclination angle ω. The unit cell width $\bar{d}$ is a fourth design variable only for the pinned configuration. The problem parameters are the applied compressive and shear stresses, $\hat{\sigma}$ and $\hat{\tau}$, and the various material properties. There are multiple inequality constraints corresponding to the failure modes: buckling and compressive yielding, and additionally, tensile yielding in the tetrahedral case. The optimisation problem

	Pyramidal	Tetrahedral	Pinned
f	$\frac{4\pi\bar{a}^2 \sec\omega}{(\sqrt{2}\tan\omega+4\bar{a})^2}$	$\frac{3\pi\bar{a}^2 \sec\omega}{(\frac{3}{2}\tan\omega+4\bar{a})(\sqrt{3}\tan\omega+4\bar{a})}$	$\frac{4\pi\bar{a}^2 \sec\omega}{\bar{d}^2}$
$\bar{\beta}$	$4\bar{E}_{fm}\bar{a}\sin\omega + \frac{2\sqrt{2}\bar{E}_{fm}\bar{a}\cos\omega}{1.1222\tan\omega}$	$4\bar{E}_{fm}\bar{a}\sin\omega + \frac{2\bar{E}_{fm}\bar{a}\cos\omega}{0.8845\tan\omega}$	$4\bar{E}_{fm}\bar{a}\sin\omega + \frac{4\bar{E}_{fm}\bar{a}\cos\omega}{1.1222\bar{d}}$
m	$\sqrt[4]{\frac{13-e}{3e}\frac{\bar{\beta}}{\pi^5\bar{a}^4\cos^4\omega}}$	$\sqrt[4]{\frac{13-e}{3e}\frac{\bar{\beta}}{\pi^5\bar{a}^4\cos^4\omega}}$	$\sqrt[4]{\frac{13-e}{3e}\frac{\bar{\beta}}{\pi^5\bar{a}^4\cos^4\omega}}$
$\hat{\sigma}_b$	$\frac{13-e}{12}\frac{\bar{\beta}}{m^2\pi^3\bar{a}^2\cos^2\omega}$	$\frac{13-e}{12}\frac{\bar{\beta}}{m^2\pi^3\bar{a}^2\cos^2\omega}$	$\frac{13-e}{12}\frac{\bar{\beta}}{m^2\pi^3\bar{a}^2\cos^2\omega}$
	$+\frac{em^2\pi^2\bar{a}^2\cos^2\omega}{4}$	$+\frac{em^2\pi^2\bar{a}^2\cos^2\omega}{4}$	$+\frac{em^2\pi^2\bar{a}^2\cos^2\omega}{4}$

Table 2: Strut arrangement-specific expressions for volume fraction f, normalized foundation modulus $\bar{\beta}$, normalized buckling stress $\hat{\sigma}_b$, and buckling mode m. The buckling mode expression is derived assuming it is a continuous variable; thus, the actual critical mode is one of the two nearest integers, whichever gives the lower buckling load. Buckling with pinned ends implies $e = 1$ while $e = 4$ for clamped ends.

is stated as follows:

$$\begin{aligned} \text{minimize} \quad & \bar{\rho} = \bar{\rho}_f(1 - f) + f \\ \text{with respect to} \quad & \bar{a}, \omega, \bar{\rho}_f, \bar{d} \\ \text{subject to} \quad & \bar{\sigma}_1 \le \bar{\sigma}_b \\ & \bar{\sigma}_1 \le \bar{\sigma}_y \\ & -\bar{\sigma}_2 \le \bar{\sigma}_y \end{aligned} \tag{26}$$

In the above problem statement, $\bar{\sigma}_2$ is negative because strut 2 must be constrained against tensile yielding in tetrahedral unit cells. Note that the unit cell thickness c does not appear because the model and optimisation problem are scale-independent; c is a parameter that must be used to obtain physical dimensions from the non-dimensional design variables after optimisation.

4.1. *Optimisation with Foam*

A grid search was used to solve the optimisation problem stated above because of the non-smoothness at the boundaries between buckling modes. A key result that is consistently observed is that *the optimal design occurs when no foam is present; that is, the foam density is zero.* The presence of foam only significantly increases the unit cell strength when the struts fail by buckling. In the buckling regime, the density of a unit cell containing both foam and struts can be reduced by decreasing the foam density and increasing the radii of the struts to compensate for the loss in buckling resistance. This remains true until the foam density reaches zero.

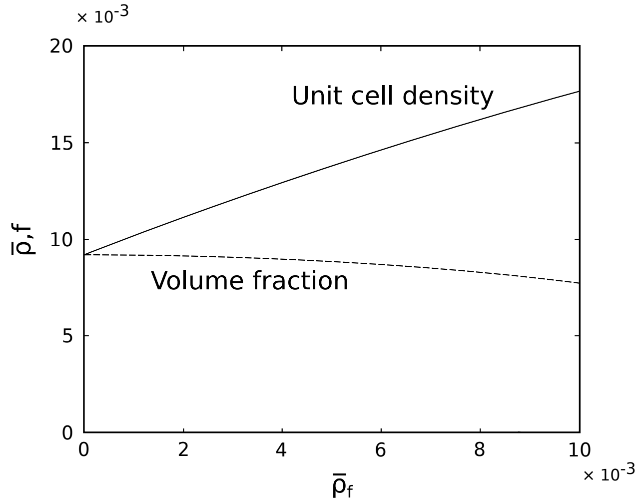

Fig. 5. Volume fraction and unit cell density at the optimum versus prescribed foam density for a pyramidal core. The applied loads are $\hat{\sigma} = 1 \times 10^{-6}$ and $\hat{\tau} = 2 \times 10^{-5}$, and titanium struts are used. Foam density is removed from the set of design variables of the original optimisation problem and treated as a parameter that is varied over a sequence of optimisation problems, illustrating the result that the optimal foam density is zero.

For illustration, Figure 5 plots the solutions from a slightly modified optimisation problem in which the unit cell density is once again minimized subject to the same failure constraints, but the foam density is a fixed parameter; thus, this modified optimisation problem yields the best design that can be achieved with a specified foam density. The volume fraction and unit cell density at the solution of the modified optimisation are plotted against a range of foam densities for a pyramidal unit cell with titanium struts under compressive and shear stresses of 0.11 MPa and 2.28 MPa, a loading that ensures potential designs fall in the buckling region where it is relevant to consider foam for the optimum unit cell. Volume fraction decreases as foam is added, lowering the mass of the struts in the unit cell; however, this is not enough to offset the density of the additional foam.

The zero foam density result is found for all combinations of compressive and shear stress for pyramidal and tetrahedral cores even when pin-joint end conditions are assumed for the strut buckling model. Moreover, because the foundation modulus is elastic and constant, the foam contribution to unit cell strength is overestimated. Despite artificially increasing the benefit of the foam, the optimisation shows that foam is an inefficient strengthening mechanism; hence this result is robust and will be replicated for more detailed models.

It follows from the zero foam density result of the pyramidal configuration that the same is true of the pinned configuration. Since $\bar{\rho}_f < 1$ is always true, the normalized unit cell density, $\bar{\rho} = \bar{\rho}_f(1 - f) + f$, always increases with volume fraction, f. As a result, increasing unit cell width, thereby reducing volume fraction, is always desirable in order to minimize the unit cell density. This observation, combined with the fact that the design space of the pyramidal core is contained within that of the pinned core, leads to the deduction that the unit cell width of the pinned optimum is greater than or equal to that of the pyramidal optimum for any given loading. Since the efficiency of foam decreases as unit cell width increases, the zero foam density result for optimal pyramidal cores implies that optimised pinned cores also do not have foam because the pinned optima have the same or higher unit cell widths, yielding the same or worse efficiency for the foam.

4.2. Optimisation with Foam Removed

A significant benefit of the zero foam density result is that the elimination of the non-differentiable regions in the strength model permits analytical solutions to the optimisation problem using the method of Lagrange multipliers. With the foam eliminated, the expressions for the stresses induced in the struts by the applied loads become

$$\sigma_1 = \frac{1}{\frac{C_1+C_2}{n} f \cos^2\omega}\left(\sigma + \frac{C_2}{C_3\tan\omega}\tau\right) \tag{27}$$

$$\sigma_2 = \frac{1}{\frac{C_1+C_2}{n} f \cos^2\omega}\left(\sigma - \frac{C_1}{C_3\tan\omega}\tau\right). \tag{28}$$

4.2.1. Pinned Configuration For the pinned unit cell, the three design variables are $\bar{a}$, $\bar{d}$, and ω, and the set of optimal designs lies in the yield region. In the buckling region, a unique minimum in $\bar{a}$-$\bar{d}$ does not exist for any strut inclination angle since the buckling resistance can be made indefinitely larger with core density fixed by increasing the strut radius and unit cell width proportionately. This is limited by the onset of yield, after which the strength cannot be increased further without an increase in density. In the yield region, both density and yield strength are functions only of the ratio $\bar{a}/\bar{d}$, meaning there are an infinite number of solutions with the same density and the required strength. However, the analytical solution presented below constrains the solution to be on the buckling-yielding boundary in order to make the unit cell as small as possible, since this means more unit cells are distributed in both directions.

The optimal pin inclination angle is decoupled from pin radius, and it can be found by solving the following implicit equation:

$$\frac{\tan\omega}{\sqrt{2}}\hat{\sigma} = \left(\frac{1}{2\sin^2\omega} - 1\right)\hat{\tau}. \tag{29}$$

With the pin angle known, it is possible to determine the pin radius to unit cell width ratio from the strength constraints. Any combination of pin radius and unit cell width that satisfies this ratio and is outside the buckling region represents a solution. The following expressions uniquely determine $\bar{a}$ and $\bar{d}$ if an additional requirement is imposed that the unit cells be as small as possible:

$$\bar{a} = \frac{\sqrt{\epsilon}}{\pi\cos\omega} \tag{30}$$

and

$$\bar{d} = \sqrt{\frac{4\pi\bar{a}^2 \cos\omega\epsilon}{\hat{\sigma} + \hat{\tau}\sqrt{2}/\tan\omega}}. \tag{31}$$

4.2.2. Pyramidal and Tetrahedral Configurations For the pyramidal and tetrahedral unit cells, the only two design variables are strut radius $\bar{a}$ and strut inclination angle ω, as the unit cell width is determined by these two variables. The key difference from the pinned configuration is that the optima are spread across multiple failure modes for different combinations of applied loads, necessitating separate analytical treatment of each of these cases.

Since both the unit cell density and strength are monotically increasing in strut radius, the constraints can never all be inactive at an optimum; one or more must always be active. For all core configurations, the single-mode failure cases (one constraint active) represent optimisation in two variables with one equality constraint while the boundary region cases (two constraints active) represent optimisation in two variables with two equality constraints. The latter type of problem has only a single feasible point; thus, it can be solved as a 2×2 nonlinear system of equations. The former type of problem can be transformed into a similar 2×2 nonlinear system using the method of Lagrange multipliers.

Pyramidal Configuration For pyramidal unit cells all feasible failure modes involve compressive yield or buckling and hence tensile yield on its own need not be considered. The optimum must be in one of three modes: buckling, compressive yield, or the buckling-yield boundary.

Figure 7(a) displays the modes in which the optimal design fails for a range of applied compressive and shear stresses. For small loads, the optimal unit cell has slender struts that fail in buckling. When the applied compressive and/or shear stresses are increased beyond this region, the buckling optima no longer satisfy the yield criterion and the yield optima do not satisfy the buckling constraint; thus, the optima lie on the boundary between buckling and compressive yielding. In this case, the struts fail simultaneously in buckling and compressive yielding. For still higher loads, the yield optima have struts that are thick enough to satisfy the buckling constraint; this is the compressive yield region.

In Figure 6, the optimal designs are represented in $\bar{a}$-ω space for increasing compressive or shear loading. The distinct regions of optima correspond exactly to those in Figure 7(a). When a pure compressive load is applied, the optima fail in buckling for loads of low magnitude or in buckling and compressive yielding simultaneously for larger loads. For shear loading, the optimal design trajectory begins in the buckling region for small loads, follows the buckling-compressive yielding boundary, and shifts to the compressive yield optima when a shear load is superimposed as the two struts in compression are loaded further.

Notable is the low sensitivity of the strut inclination angle to the magnitude of loading for the buckling and yield optima. If a pyramidal or tetrahedral core is to be designed for strictly shear loads of any magnitude or strictly compressive loads below a certain magnitude, the optimal strut inclination angles are roughly $\sim 40°$ and $45° \sim 50°$, respectively, giving a simple heuristic for design.

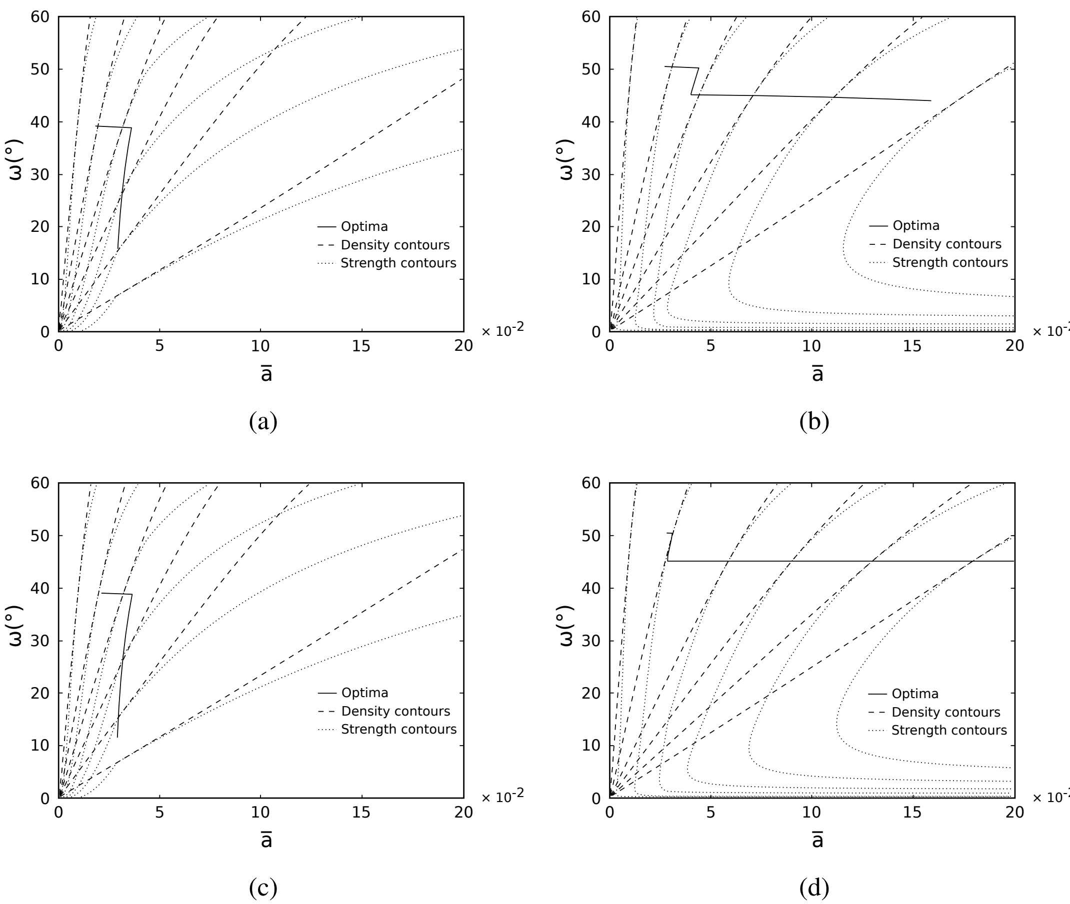

Fig. 6. Optimal design trajectories for a pure compressive load on a pyramidal unit cell (a), a pure shear load on a pyramidal unit cell (b), a pure compressive load on a tetrahedral unit cell (c), and a pure shear load on a tetrahedral unit cell (d), plotted over density and strength contours. The struts in each case are assumed to be made of titanium. The abrupt changes in the optimal design trajectories indicate transitions between modes in which the optimal designs fail. For compression, the optimal design trajectory begins in the buckling region and transitions to the buckling-yield boundary as the applied load increases. For the pyramidal unit cell under shear loading, the optima begin in the buckling region and eventually transition to the compressive yield region while for the tetrahedral unit cell under shear loading, the optima begin in the buckling region and transition to the tensile yield region for larger loads.

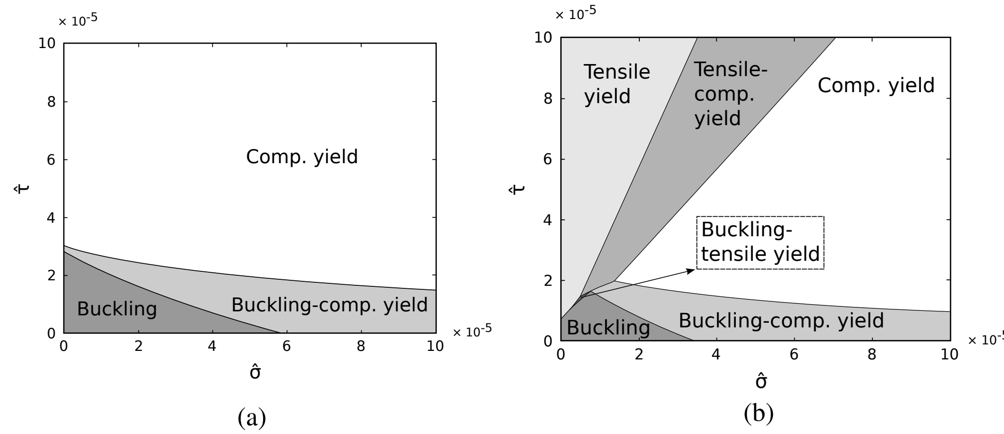

Fig. 7. Failure mode map of the optima in $\hat{\sigma}$-$\hat{\tau}$ space for the pyramidal (a) and tetrahedral (b) configurations with titanium struts.

Tetrahedral Configuration Tetrahedral unit cells differ from their symmetric cousins because they may yield in tension, giving six total failure mechanisms: buckling, compressive yield, tensile yield, simultaneous buckling and compressive yield, simultaneous buckling and tensile yield, and simultaneous compressive yield and tensile yield. For a predominantly compressive loading on a tetrahedral unit cell, the failure modes of interest are equivalent to those for the pyramidal configuration. With shear loading, the possibility of the lone strut in tension yielding introduces three additional regions of optima as illustrated in the failure mode map in Figure 7(b). For high shear loads with negligible compressive loads, the dominant failure mode is tensile yielding of the lone strut; however, when the compressive load is increased the optimum shifts to a region in which the strut in tension and the struts in compression all yield simultaneously. For yet higher compressive loads, the combined application of compression and shearing has a cancelling effect on the stress in the lone strut, but an additive one on the stresses in the two in compression: this shifts the optima back to the compressive yielding region.

4.3. Comparison Between Configurations

Figures 8 and 9 plot contours of unit cell density, strut radius, and strut inclination angle at the optimum point for the pyramidal, tetrahedral, and pinned cores. The existence of multiple failure regions for the pyramidal and tetrahedral configurations is the cause for non-smoothness in certain regions, while the contours for the pinned cores are smooth everywhere because their optima fall in a single region. The contour plot corresponding to the tetrahedral configuration is not monotonic with respect to $\hat{\sigma}$ and $\hat{\tau}$ because applying a compressive stress in the presence of a shear load improves the efficiency of the unit cell by reducing the load on the strut experiencing tension. For a tetrahedral unit cell that is optimally designed in this region, the loading history becomes as important as the final loading condition since the compressive load must be applied first, followed by the shear load: otherwise, the strut in tension would fail during loading.

Comparing optimally designed unit cells, for the large majority of compressive and shear strength combinations the tetrahedral configuration is the most efficient. For high shear strengths and low compressive strengths, pinned and pyramidal unit cells are equally optimal, while pinned unit cells alone have the lowest mass for low shear strengths and high compressive strengths. A full map of optimal configurations is shown in Figure 10.

The tetrahedral unit cell is superior to the pinned and pyramidal unit cells in most cases because it has a larger unit cell area and one less strut, yielding a reduction in volume fraction — roughly $\sim \frac{1}{\sqrt{3}}$ — that outweighs the reduction in yield strength for the majority of loading combinations. The loss in efficiency due to having two struts oriented 60° to the direction of the shear force is regained by the strut oriented parallel to the shear force, whereas the four struts in a pyramidal unit cell have a 45° orientation.

This trade-off does not apply when one of the applied compressive or shear stress is much lower than the other. When the loading is nearly pure compression, a pinned core with a large unit cell width is the most efficient. As long as there is little or no shear force applied, the pinned core can maintain vertical or nearly vertical pins without buckling at a fixed volume fraction by increasing the pin radius and unit cell width while holding their ratio constant. When the loading is nearly pure shear, the tetrahedral core is less efficient than the pyramidal and pinned cores because the critical strut carries twice the load of the other two struts. The tetrahedral unit cell is oriented such that one strut is in tension and two are in compression to delay buckling; however, when the loading is primarily shear, the dominant failure mode is tensile yielding of the lone strut. Increasing the applied compressive stress lightens the optimal unit cell by reducing the tensile load on the strut.

In this region, the densities of the optimal pinned and pyramidal unit cells are equal to each other. The reason is that a high shear strength constraint necessitates a large inclination angle such that the optimal pyramidal unit cell lies in the yield region. The large strut inclination angle results in a large unit cell, requiring a thicker strut that yields before it buckles. Since pinned and pyramidal unit cells are equivalent in the yield region, they are equally optimal for high shear and low compressive stresses.

5. Conclusion

This work presents the qualitative characteristics of lightweight hybrid unit cells for sandwich structures. Models were developed for stress analysis of the unit cell as well as prediction of strut buckling for multiple core configurations. These were optimised to explore the effect of core configuration and geometric parameters in the design of a unit cell that can simultaneously carry shear and compressive loads with the minimum mass. The results can be summarized by three conclusions.

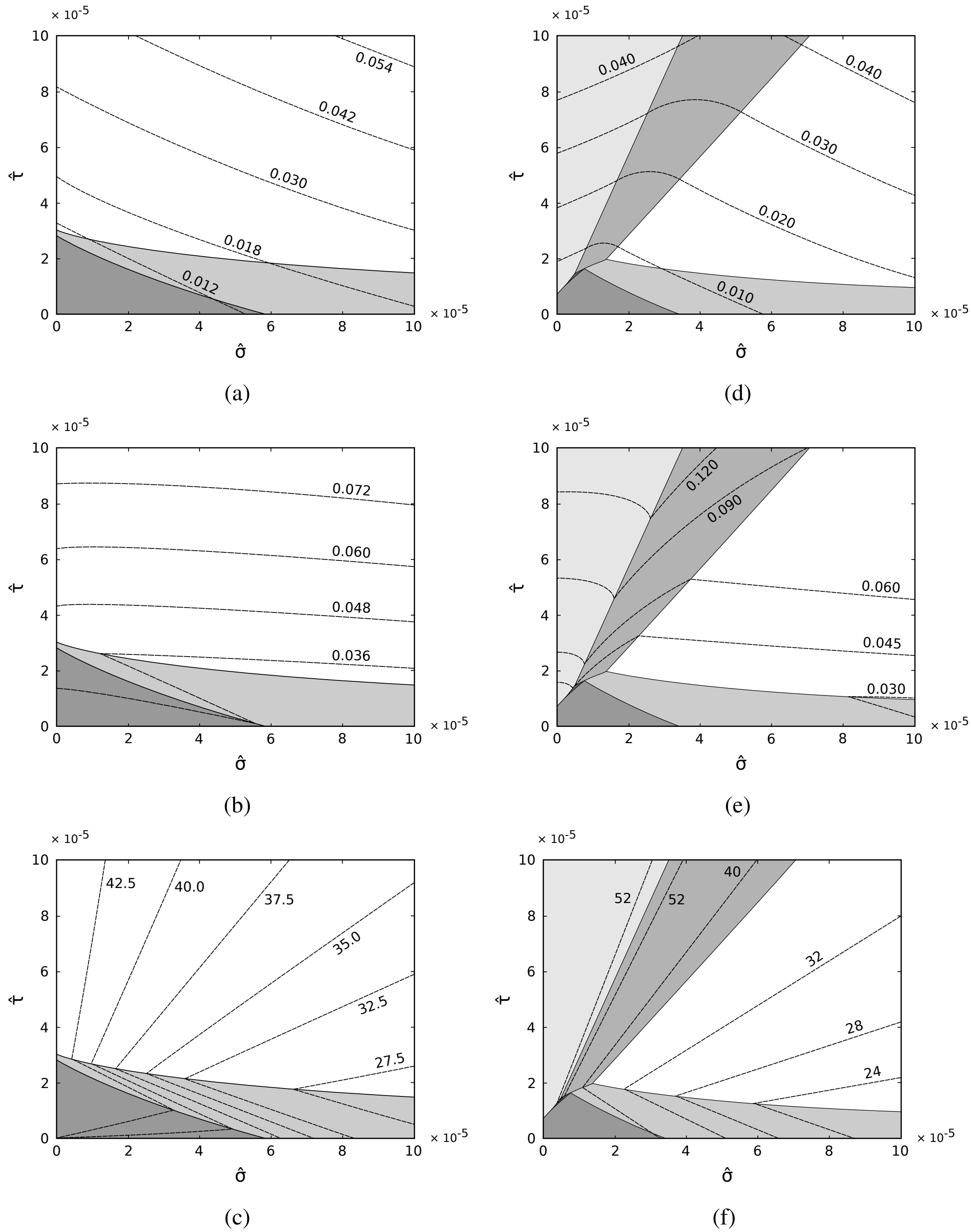

Fig. 8. Contour plots in $\hat{\sigma}$-$\hat{\tau}$ space for the objective function ((a),(d)), strut radius ((b),(e)), and strut inclination angle ((c),(f)) corresponding to the optimal unit cell with titanium struts. (a), (b), and (c) represent the pyramidal configuration, while (d), (e), and (f) represent the tetrahedral configuration.

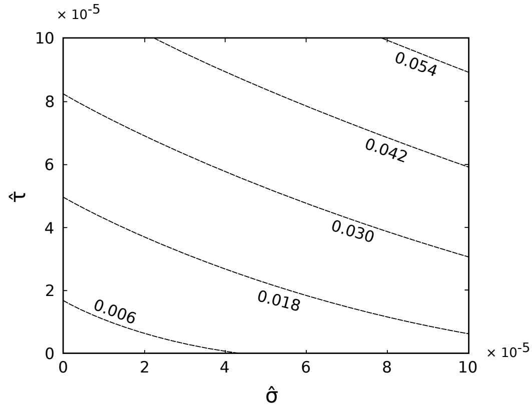

(a)

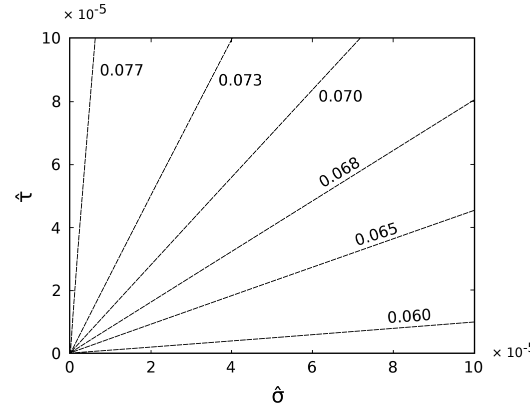

(b)

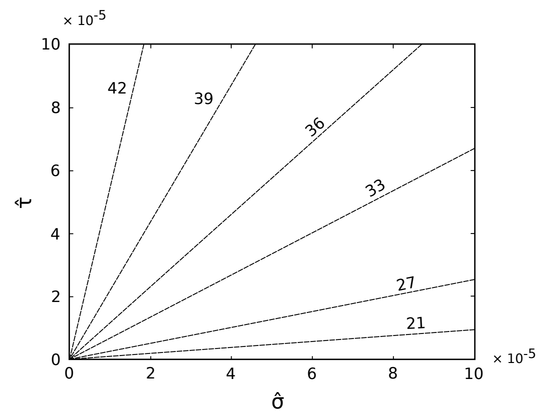

(c)

Fig. 9. Contour plots in $\hat{\sigma}$-$\hat{\tau}$ space for the objective function (a), strut radius (b), and strut inclination angle (c) corresponding to the optimum design for the pinned configuration.

First, despite a model that overestimates the foam's suppression of strut buckling, the optimised cores for pyramidal, tetrahedral, and pinned configurations *do not contain any foam*.[1] This is a result that contradicts some previous studies; however, when optimised, the unit cell consisting of struts and no foam has a lower mass than can be achieved with any hybrid foam-strut unit cell. As a result, all further work uses an analysis without foam, enabling the development of analytical, though not closed-form, optimisation solutions.

The second major finding is that for predominantly shear loading, which is common in sandwich beam applications, the optimal inclination angle of the struts or pins is between roughly 45° and 50° for a broad

[1] Additional unpublished calculations on corrugated configurations showed that, similar to [28], the advantage of removing the foam from the corrugated configuration was not strong.

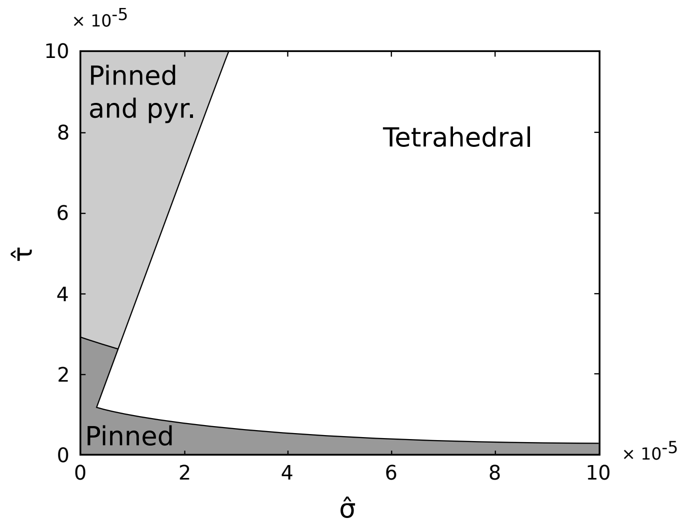

Fig. 10. Plot showing the most efficient core configuration for combinations of $\hat{\sigma}$ and $\hat{\tau}$. The pinned configuration is optimal for predominantly compressive loading, the pyramidal and pinned configurations are equally optimal for predominantly shear loading, and the tetrahedral configuration is optimal for relatively large compressive and shear loads.

range of magnitudes of the applied shear stress, regardless of the mode of failure. For predominantly compressive loading, the optimal inclination angle is approximately 40° when the optimum is in the buckling region.

Finally, the tetrahedral configuration is the most efficient for the majority of combined loading scenarios. When a combination of a compressive and a shear stress, both of significant magnitude, is applied, the tetrahedral unit cell benefits from the reduction of mass from having one fewer strut, with two in compression and one in tension. The tensile stress in the lone strut is reduced because the effects of the applied compressive and shear stresses cancel each other to an extent. For predominantly compressive loading, the pinned core with large unit cells and nearly vertical pins is the most efficient, and for predominantly shear loading, the pinned and pyramidal cores in compressive yielding are equally optimal.

Acknowledgments

The authors gratefully acknowledge financial support from the University of Toronto, the University of Michigan, and the Natural Sciences and Engineering Research Council of Canada (NSERC).

References

[1] F J Plantema. *Sandwich Construction*. John Wiley and Sons, New York, 1966.

[2] H G Allen. *Analysis and Design of Structural Sandwich Panels*. Pergamon Press, Oxford, 1969.

[3] D Zenkert. *An Introduction to Sandwich Construction*. Engineering Materials Advisory Service, Sheffield, U.K., 1995.

[4] D D Cartié and N A Fleck. The effect of pin reinforcement upon the through-thickness compressive strength of foam-cored sandwich panels. *Composites Science and Technology*, 63(16):2401–2409, December 2003.

[5] V S Deshpande and N A Fleck. Collapse of truss core sandwich beams in 3-point bending. *International Journal of Solids and Structures*, 38(36-37):6275–6305, September 2001.

[6] H-L Fan, T Zeng, D-N Fang, and W Yang. Mechanics of advanced fiber reinforced lattice composites. *Acta Mechanica Sinica*, 26(6):825–835, December 2010.

[7] I K Partridge, D D R Cartié, and T Bonnington. Manufacture and performance 0f Z-pinned composites. In S Advani and G Shonaike, editors, *Advanced polymeric materials: structure-property relationships*, chapter 3. CRC Press, 2003.

[8] H N G Wadley, N A Fleck, and A G Evans. Fabrication and structural performance of periodic cellular metal sandwich structures. *Composites Science and Technology*, 63(16):2331–2343, 2003.

[9] J E Campbell, F Forte, G D Hibbard, and H E Naguib. Periodic cellular metal / polyurethane foam hybrids. *Journal of Composite Materials*, 43(3):207–216, February 2009.

[10] H Denli and J Q Sun. Structural-acoustic optimization of sandwich structures with cellular cores for minimum sound radiation. *Journal of Sound and Vibration*, 301(1-2):93–105, March 2007.

[11] C J Yungwirth, H N G Wadley, J H O'Connor, A J Zakrasyek, and V S Deshpande. Impact response of sandwich plates with a pyramidal lattice core. *International Journal of Impact Engineering*, 35(8):920–936, 2008.

[12] T J Lu, L Valdevit, and A G Evans. Active cooling by metallic sandwich structures with periodic cores. *Progress in Materials Science*, 50(7):789–815, September 2005.

[13] M A Dweib, B Hu, A O'Donnell, H W Shenton, and R P Wool. All natural composite sandwich beams for structural applications. *Composite Structures*, 63(2):147–157, February 2004.

[14] F Cote, N A Fleck, and V S Deshpande. Fatigue performance of sandwich beams with a pyramidal core. *International Journal of Fatigue*, 29(8):1402–1412, August 2007.

[15] J C Wallach and L J Gibson. Mechanical behavior of a three-dimensional truss material. *International Journal of Solids and Structures*, 38(40-41):7181–7196, October 2001.

[16] N Wicks and J W Hutchinson. Optimal truss plates. *International Journal of Solids and Structures*, 38(30-31):5165–5183, July 2001.

[17] N Wicks and J W Hutchinson. Performance of sandwich plates with truss cores. *Mechanics of Materials*, 36(8):739–751, August 2004.

[18] J-S Liu and T J Lu. Multi-objective and multi-loading optimization of ultralightweight truss materials. *International Journal of Solids and Structures*, 41(3-4):619–635, February 2004.

[19] T Liu, Z C Deng, and T J Lu. Design optimization of truss-cored sandwiches with homogenization. *International Journal of Solids and Structures*, 43(25-26):7891–7918, December 2006.

[20] E Dragoni. Optimal mechanical design of tetrahedral truss cores for sandwich constructions. *Journal of Sandwich Structures and Materials*, 15(4):464–484, 2013.

[21] L Du, G-Q Jiao, and T Huang. The Elastic Properties of Sandwich Structure with Z-pinned Foam Core. *Journal of Reinforced Plastics and Composites*, 28(7):813–831, April 2009.

[22] L J Gibson and M F Ashby. *Cellular Solids, second edition*. Cambridge University Press, Cambridge, 1997.

[23] B T Bhat and T G Wang. A comparison of mechanical properties of some foams and honeycombs. *Journal of Materials Science*, 25(12):5157–5162, November 1990.

[24] S P Timoshenko and J M Gere. *Theory of Elastic Stability*. McGraw Hill, New York, 2nd edition, 1961.

[25] G Zingone. Limit analysis of a beam in bending immersed in an elasto-plastic medium. *Meccanica*, 3:48–56, 1968.

[26] T Liu, Z C Deng, and T J Lu. Analytical modeling and finite element simulation of the plastic collapse of sandwich beams with pin-reinforced foam cores. *International Journal of Solids and Structures*, 45(18-19):5127–5151, September 2008.

[27] M Hetenyi. *Beams On Elastic Foundation*. University of Michigan Press, Ann Arbor, 1979.

[28] A Vaziri, Z Xue, and J W Hutchinson. Metal sandwich plates with polymer foam-filled cores. *Journal of Mechanics of Materials and Structures*, 1(1):97–127, 2006.